

Supramolecular Organolead(IV) and -tin(IV) Systems $[(\text{Me}_3\text{E}^{\text{IV}})_3\text{M}^{\text{III}}(\text{CN})_6]_\infty$ (E = Pb or Sn, M = Co or Fe): Comparative X-ray Diffraction and Solid-State Multinuclear Magnetic Resonance Studies

Ulrich Behrens, Abdul K. Brimah, Tarek M. Sollman,[†] and R. Dieter Fischer*

Institut für Anorganische und Angewandte Chemie, Universität Hamburg, Martin-Luther-King-Platz 6,
 W-2000 Hamburg 13, FRG

David C. Apperley, Nicola A. Davies, and Robin K. Harris*

Department of Chemistry, University of Durham, South Road, Durham DH1 3LE, U.K.

Received October 30, 1991

The synthesis of two novel 3D coordination polymers $[(\text{Me}_3\text{Pb}^{\text{IV}})_3\text{M}^{\text{III}}(\text{CN})_6]_\infty$ with M = Co (4) and Fe (5) is described together with features of their vibrational spectra. Compound 4 was successfully subjected to a single-crystal X-ray study, the results of which have in turn initiated a reinspection of the structure of the tin homologue, 1, based upon the more appropriate space group $P2_1/c$ (rather than $C2/c$). The lattice of 4 corresponds, like that of 1, to a three-dimensional polymeric network. The structure with the space group $P2_1/c$ ($Z = 4$) and $a = 16.370$ (4) Å, $b = 12.727$ (3) Å, $c = 14.263$ (4) Å, and $\beta = 104.69$ (2)° was refined to $R = 0.060$ for 1598 reflections ($F_o > 6\sigma(F_o)$). The nonsuperimposable 3D networks of 1 and 4 involve $\text{Me}_3\text{E}(\text{NC})_2$ units (E = Sn or Pb) of trigonal-bipyramidal configuration and remarkably wide, practically parallel channels whose walls are internally coated by constituents of the lipophilic Me_3E groups. The presence of three crystallographically nonequivalent chains, $[-\text{Co}-\text{C}\equiv\text{N}-\text{E}-\text{N}\equiv\text{C}-]_\infty$, in the lattices of both 1 and 4 has initiated detailed cross-polarization magic-angle spinning (CP MAS) solid-state NMR studies involving the nuclei ^{13}C , ^{15}N , ^{59}Co , ^{207}Pb , or ^{119}Sn with a view to establishing structure/NMR correlations. Quite unexpectedly, the CP NMR spectra would favor more symmetrical structures than the X-ray diffraction (XRD) results. The deductions drawn from the NMR spectra in total allow valuable predictions about the structural details of related polymers which are still inaccessible to single-crystal X-ray studies. The $\delta(^{207}\text{Pb})$ values of the *tpb*-configured $\text{Me}_3\text{Pb}(\text{NC})_2$ units of 4 (78 and 172 ppm) are still more positive than the shift of the tetrahedral reference sample Me_4Pb .

Introduction

The long-pending expectation that compounds of the composition $[(\eta^5\text{-Cp})_3\text{U}^{\text{IV}}]_3\text{M}^{\text{III}}(\text{CN})_6$ (Cp = C_5H_5) and $[(\text{R}_3\text{Sn}^{\text{IV}})_3\text{M}^{\text{III}}(\text{CN})_6]$, respectively (R = alkyl or aryl, and M = e.g. Fe or Co), could represent a novel class of organometallic 3D polymers^{1,2} was confirmed first in 1985 by the fortuitous preparation of single crystals of the strongly insoluble representative with R = Me and M = Co (1), followed by a successful X-ray diffraction study.³ The lattice of 1 is in fact a 3D network of regularly interlinked, infinite $[-\text{Co}-\text{C}\equiv\text{N}-\text{Sn}-\text{N}\equiv\text{C}-]_\infty$ chains displaying ample, straight channels (with a cross-section of about 10×10 Å²) whose internal surfaces are efficiently coated by atoms of the methyl ligands of the Sn atoms.⁴ This unprecedented⁵ mode of supramolecular architecture differs, however, from an initially envisaged,² even less compact, "super-Prussian-blue" (SPB) network which would involve a single type of strictly linear chains oriented along each of the three Cartesian axes. The actual structure of 1 differs, however, also from those of the purely inorganic polymers like $[\text{H}_3\text{Co}(\text{CN})_6]_\infty$,⁶ $[\text{Ag}_3\text{Co}(\text{CN})_6]_\infty$,⁷ etc. (vide infra).

The availability of notably large cavities within the novel organometallic polymers can also be demonstrated chemically^{4,8,9} by the facile encapsulation of voluminous organic and organometallic guest cations G^{n+} into e.g. the negatively charged host lattice $[(\text{Me}_3\text{Sn})_3\text{Fe}^{\text{II}}(\text{CN})_6]^-$ formally accessible by complete reduction of the isostructural iron homologue $[(\text{Me}_3\text{Sn}^{\text{IV}})_3\text{Fe}^{\text{III}}(\text{CN})_6]_\infty$ (2) of 1. The crystal structures of two such zeolite-like 3D host-guest systems:

$[\text{G}^{n+}_{1/n}(\text{Me}_3\text{Sn}^{\text{IV}})_3\text{M}^{\text{II}}(\text{CN})_6]^-$ (with $\text{G}^{n+}_{1/n} = 1/2(\text{methylviologen}^{2+})$, M = Ru,⁹ and Cp_2Co^+ , M = Fe,^{10,11} respectively) have so far been fully characterized.

Meanwhile various guest-free homologues of 1 and 2 were prepared in which either the organic group R of the R_3Sn component is modified^{1,2,3,11,12} or M = Fe is replaced

(1) Yünlü, K. Doctoral Dissertation, Universität Hamburg, Germany, 1983; p 88. See also: Siemel, G. R. Doctoral Dissertation, Universität Erlangen-Nürnberg, Germany, 1976; p 77. Fischer, R. D.; Siemel, G. R. *J. Organomet. Chem.* 1978, 156, 383.

(2) Uson, R.; Fornies, J.; Uson, M. A.; Lalinde, E. *J. Organomet. Chem.* 1980, 185, 359.

(3) Yünlü, K.; Höck, N.; Fischer, R. D. *Angew. Chem.* 1985, 97, 863; *Angew. Chem., Int. Ed. Engl.* 1985, 24, 879.

(4) Brandt, P.; Brimah, A. K.; Fischer, R. D. *Angew. Chem.* 1988, 100, 1578; *Angew. Chem., Int. Ed. Engl.* 1988, 27, 1521.

(5) The novel, most essential feature characterizing the title compounds is the presence of the organometallic "spacer" component, R_3E^+ , between two cyanide N atoms; for remotely related 3D polymers devoid of such spacer units, see: (a) Hoskins, B. F.; Robson, R. *J. Am. Chem. Soc.* 1990, 112, 1546. (b) Abrahams, B. F.; Hoskins, B. F.; Liu, J.; Robson, R. *J. Am. Chem. Soc.* 1991, 113, 3045. (c) Abrahams, B. F.; Hoskins, B. F.; Robson, R. *J. Am. Chem. Soc.* 1991, 113, 3606.

(6) (a) Güdel, H. U.; Ludi, A.; Fischer, P. *J. Chem. Phys.* 1972, 56, 675. (b) Haser, R.; de Broin, C. E.; Pierrot, M. *Acta Crystallogr.* 1972, B28, 2530. (c) Beck, W.; Smedal, H. S. *Z. Naturforsch.* 1965, 20B, 109.

(7) Ludi, A.; Güdel, H. U. *Helv. Chim. Acta* 1968, 51, 1762.

(8) Eller, S.; Brandt, P.; Brimah, A. K.; Schwarz, P.; Fischer, R. D. *Angew. Chem.* 1989, 101, 1274; *Angew. Chem., Int. Ed. Engl.* 1989, 28, 1263.

(9) Eller, S.; Adam, M.; Fischer, R. D. *Angew. Chem.* 1990, 102, 1157; *Angew. Chem., Int. Ed. Engl.* 1990, 29, 1126.

(10) Schwarz, P.; Brimah, A. K.; Behrens, U.; Fischer, R. D.; Nolte, U. Unpublished results.

(11) Apperley, D. C.; Davies, N. A.; Harris, R. K.; Brimah, A. K.; Eller, S.; Fischer, R. D. *Organometallics* 1990, 9, 2672.

(12) Bonardi, A.; Carini, C.; Pelizzi, C.; Pelizzi, G.; Predieri, G.; Tarasconi, P.; Zoruddu, M. A.; Molloy, K. C. *J. Organomet. Chem.* 1991, 401, 283.

[†]Ultimate address: Department of Chemistry, Faculty of Science, Tanta University, Tanta, Egypt.

Table I. Representative Spectroscopic (IR/Raman) Data for Various $[A_3Co(CN)_6]_\infty$ Polymers

A	$\nu(CN)$			$\nu(SnC)/\nu(PbC)$		$\nu(CoC)$ (IR)
	IR (t_{1g}) ^a	Ra (e.g. a_{1g}) ^{b,c}		IR (asym)	Ra (sym/asym) ^b	
Et ₄ N	2112 (2118) 2123 (sh)	2123	2135			405
K ^{6c}	2118 (2105)	2137	2150			414
Me ₃ Pb	2127 (2117) 2131 (sh)	2147	2169	496	472, 500 (w)	424
Bu ₃ Sn	2149	2166	2181	462	516	425
Et ₃ Sn	2156	2185	2190	526	498, 525 (w)	434
Me ₃ Sn ³	2158 (2140) 2168 (sh)	2180	2195	554	524, 556 (w)	438
Ag	2187 (2170)	2190	2209			486/493
H ^{6c}	2218 (2113)	2165 (sh)	2220 (br)			420

^a In parentheses, $\nu(CN)$ of corresponding $[A_3Fe^{III}(CN)_6]$ system. ^b Raman active. ^c Measurements from our laboratory.

by its higher homologues Ru and Os.¹³ However, comparatively few attempts to vary the central metal E of the organometallic R₃E fragment have been made. So far, only some mixed-M/R₃ polymers, $[(Me_3Sn^{IV})_2(Me_3Sb^V)M^{II}(CN)_6]_\infty$ (M = Fe, 3; M = Ru, 3a), have been described.¹⁴ Hence, in the present contribution, the organolead(IV) homologues of 1 (M = Co, 4) and 2 (M = Fe, 5) will be reported¹⁵ and compared in detail with 1 and 2. In view of the rather promising perspectives to be drawn from the results of a recent solid-state NMR study of various polymeric $[(R_3Sn)_mM(CN)_m]_\infty$ systems,¹¹ the present study is accompanied by an extended CP MAS NMR investigation covering the nuclei ¹³C, ¹⁵N, ⁵⁹Co, ²⁰⁷Pb, and ¹¹⁹Sn, respectively, of 1, 4, and a number of related diamagnetic compounds $[A_3Co(CN)_6]$. Of course, 2 and 5 are paramagnetic, so high-resolution NMR studies of these systems are not feasible.

Preparation, Chemical Properties, and Vibrational Spectra of the $[(Me_3Ph)_3M(CN)_6]_\infty$ System (M = Co, 4; M = Fe, 5)

Precipitates of diamagnetic, white 4 and paramagnetic, orange 5 (effective magnetic moment ca. 2.11 μ_B), respectively, are obtained in yields of up to 80% when saturated aqueous solutions of Me₃PbCl are added to concentrated solutions of K₃[M(CN)₆]. As 4 and 5 dissolve in H₂O notably better than their Me₃Sn homologues, 1 and 2, the otherwise instantaneous, complete precipitation of polycrystalline 4 and 5 can be circumvented by sufficient dilution of the starting solutions. Hence, well-shaped crystals of both compounds become accessible even more readily than, e.g., crystals of 1 from H₂O/THF mixtures.³ The better solvation of 4 and 5 in H₂O is paralleled by notably lower thermal stabilities of the solid samples, pure 4 decomposing above 230 °C (5, ca. 200 °C), while 1 remains unchanged up to 335 °C (2, ca. 220 °C). In sunlight, compound 5 undergoes continuous decomposition (although somewhat less rapidly than 2¹⁶), the nature of the resulting yellow, almost diamagnetic materials being still ill-defined. The vibrational spectra in the $\nu(CN)$ absorption range (completely light-covered 5: $\nu(CN)$ 2072 (s), 2060 (s), 2042 (s)) suggest that the redox reaction $Fe^{III}(CNE)_6 \rightleftharpoons Fe^{II}(CNE)_6$ (E = Pb or Sn) has taken place, but

the nature of the electron donor is still unclear.

Freshly prepared 5 can, like 2, be transferred into several probably zeolite-like host-guest systems $[G^+_{x-}(Me_3Pb^{IV})_3Fe^{III}_{1-x}Fe^{II}_x(CN)_6]_\infty$ ($0 \leq x \leq 1$), mainly by tribochemical reaction at room temperature with the corresponding iodides, GI ($G^+ =$ e.g. Et₄N⁺, Cp₂Fe⁺, K⁺, etc.),¹⁷ and moreover, with unsaturated heterocyclic π -electron donors like pyrroles, pyridines, etc.¹⁸ In contrast to, e.g., (Et₄N)I and KI, which react with 5 only incompletely under grinding, the tribochemical reaction of 5 (and likewise of 2) with Cp₂FeI turns out to be complete within about 15 min. The apparently new, dark green reactant (Cp₂Fe)I is easily obtained by grinding mixtures of equivalent quantities of sublimed ferrocene and iodine and offers several advantages over the application of, e.g., black (Cp₂Fe)I₃¹⁹ or neat Cp₂Fe.⁴

While both 4 and 5 display $\nu(PbC)$ absorptions with wavenumbers very close to those of common (both pseudo- T_d - and tbp -configured) Me₃PbX systems²⁰ (cf. Table I), more detailed comparison of the IR and Raman spectra of 4 and 5 lends support of tbp configuration. Under high resolution in the $\nu(CN)$ range, only the IR spectra of, e.g., 1³ and 4 display more than one absorption which is likely to reflect the significantly perturbed surroundings of their Me₃E-interlinked Co(CN)₆ octahedra (vide infra). Interestingly, the polymers $[(R_3Sn)_3Co(CN)_6]_\infty$ with R = Et and Bu², respectively, which also give rise to somewhat simpler ¹³C, ¹⁵N, and ¹¹⁹Sn, solid-state NMR spectra,¹¹ show only one sharp and symmetrical $\nu(CN)$ absorption. The individual band positions of the various polymers $[A_3Co(CN)_6]_\infty$ listed in Table I exceed those of the "parent" salts (with A = K and Et₄N) gradually, reflecting probably the actual amount of nonelectrostatic interaction^{22b} between the cyanide N atoms and A⁺. Thus $\nu(CN)$ increases along the sequence Et₄N⁺ < K⁺ < Me₃Pb⁺ < Me₃Sn⁺ < H⁺ < Ag⁺. The increase of $\nu(CN)$ for A = Me₃Pb (relative to solid K₃[Co(CN)₆]) is comparable in magnitude with that observed for aqueous solutions of K₃[Co(CN)₆] in the absence and presence, respectively, of mineral acids.²¹ The wavenumber of the IR-active $\nu(CoC)$ vibration increases along with that of $\nu(CN)$, suggesting that the anticipated, gradual "reorientation" of the partially π -antibonding ("lone") electron pair on each cyanide N atom toward a suitable vacant orbital of the Lewis acid A⁺ could be ac-

(13) Eller, S.; Fischer, R. D. *Inorg. Chem.* 1990, 29, 1289. Moreover, the rhodium homologue of 1 has been prepared: Eller, S.; Fischer, R. D. Unpublished results.

(14) (a) Eller, S.; Dülse, S.; Fischer, R. D. *J. Organomet. Chem.* 1990, 390, 309. (b) Eller, S.; Schaugsdat, S.; Fischer, R. D. Unpublished results.

(15) To the best of our knowledge, compound 4 was prepared first, and analyzed correctly, in 1985: Yünlü, K.; Fischer, R. D. Unpublished results.

(16) Brandt, P.; Fischer, R. D.; Sanchez Martinez, E.; Diaz Calleja, R. *Angew. Chem.* 1989, 101, 1275; *Angew. Chem., Int. Ed. Engl.* 1989, 28, 1265.

(17) Brimah, A. K.; Soliman, T. M.; Schwarz, P.; Fischer, R. D. Unpublished results.

(18) (a) Etaiw, S. E. H.; Soliman, T. M.; Fischer, R. D.; Brandt, P. To be published. (b) Ibrahim, A. M. A.; Etaiw, S. E. H.; Soliman, T. M. *J. Organomet. Chem.*, in press.

(19) Nese, E. W.; Loonat, M. S. *J. Organomet. Chem.* 1985, 286, 329.

(20) Clark, R. J. J.; Davies, A. G.; Puddephatt, R. J. *J. Am. Chem. Soc.* 1968, 90, 6923.

(21) Eaton, D. R.; Sandercock, A. C. *J. Phys. Chem.* 1982, 86, 1371.

Table II. Selected Crystal Data for 1 and 4

	$[(\text{Me}_3\text{Sn})_3\text{Co}(\text{CN})_6]_\infty$ (1)	$[(\text{Me}_3\text{Pb})_3\text{Co}(\text{CN})_6]_\infty$ (4)
formula	$\text{C}_{15}\text{H}_{27}\text{N}_6\text{CoSn}_3$	$\text{C}_{15}\text{H}_{27}\text{N}_6\text{CoPb}_3$
mass of formula unit (M_f), g/mol	706.5	971.9
cryst syst	monoclinic	monoclinic
space group	$P2_1/c$	$P2_1/c$
a , Å	16.857 (6)	16.370 (4)
b , Å	12.941 (7)	12.727 (3)
c , Å	14.664 (5)	14.263 (4)
β , deg	106.99 (3)	104.69 (2)
V , Å ³	3059 (3)	2874.4 (13)
Z	4	4
$d(\text{calcd})$, g/cm ³	1.534	2.246
$F(000)$	1344	1728
μ , cm ⁻¹	28	175 ²⁴
cryst size, mm	a	$0.2 \times 0.2 \times 1.2$
$2\theta_{\text{max}}$, deg (Mo K α)	5–50	5–47.5
total no. of data	5937	3883
total no. of unique data	5290	3635
no. of obsd data [$F > \sigma(F)$]	1914 ($n = 3$)	1598 ($n = 6$)
no. of refined params	229	214
weighting scheme	unit weights	$w = [\sigma^2(F) + 0.0003F^2]^{-1}$
final R ; R_w	0.101; 0.091	0.060; 0.059

^a Not recorded.

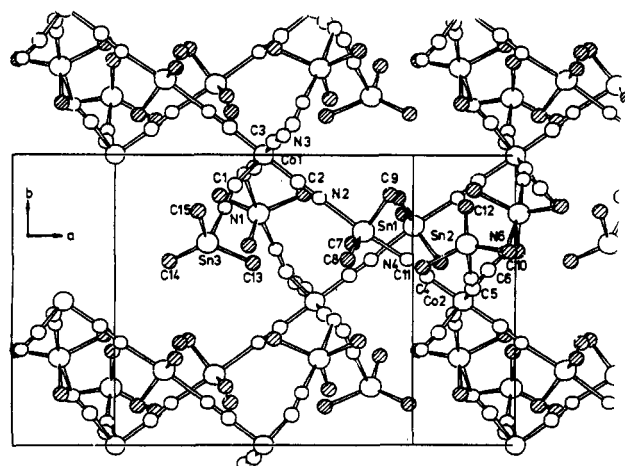
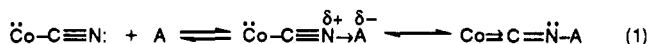


Figure 1. Elementary cell and atomic numbering scheme (of the asymmetric unit) of $[(\text{Me}_3\text{Sn})_3\text{Co}(\text{CN})_6]_\infty$ (1). Shaded circles represent methyl carbon atoms.

accompanied by a concomitant increase of $\text{Co} \rightarrow \text{C}$ π -electron back-donation.²²



Crystal Structure of 4 and Reinspection of the Structure of 1

While the light-sensitivity of 5 makes this compound rather unfavorable for detailed X-ray diffraction studies, the "X-ray quality" of a carefully selected crystal of 4 turned out to even exceed that of the crystal of 1 examined in 1985,³ in spite of a large, inevitable X-ray absorption due to the high lead content of 4. Thus, during the determination of the structure of 4, it has become evident that its space group $P2_1/c$ would also account for the structure of 1, and that the earlier-adopted space group $C2/c$ is inadequate. In fact, there has been evidence of additional, rather weak peaks on the X-ray films of 1, suggesting a primitive space group. The virtually more

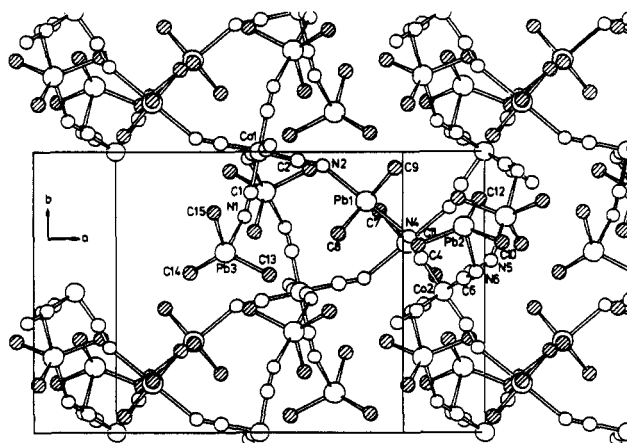


Figure 2. Elementary cell and atomic numbering scheme (of the asymmetric unit) of $[(\text{Me}_3\text{Pb})_3\text{Co}(\text{CN})_6]_\infty$ (4). Shaded circles represent methyl carbon atoms.

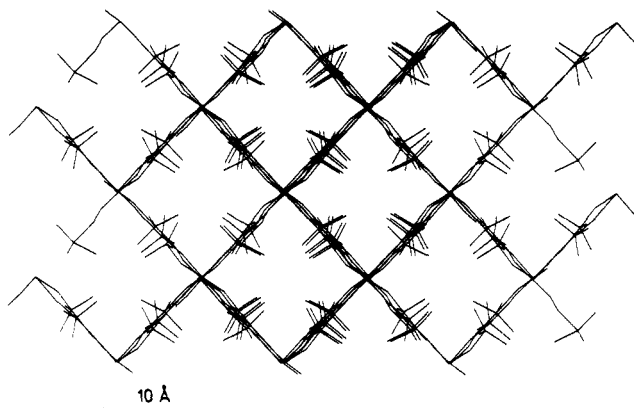


Figure 3. Lattice of 1; view along the main channels, i.e. [101].

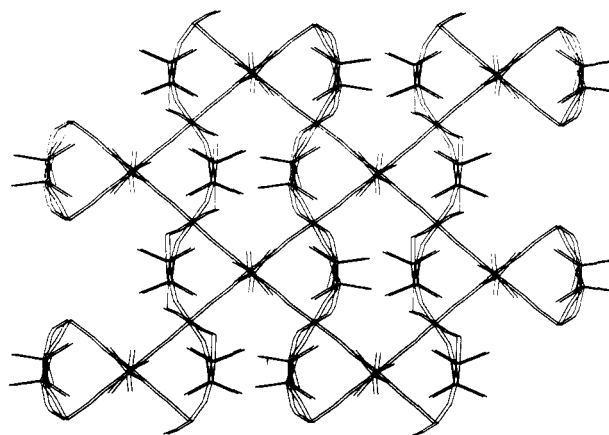


Figure 4. Lattice of 1; viewed along c , [001] (see also Figure 1).

favorable R value of 0.078 from the initial treatment³ in $C2/c$ reflects the fact that these weak reflections are less significant for the treatment in $C2/c$ than in $P2_1/c$ symmetry. In the following, only the results of a reexamination of the structure of 1, based on the already deposited, truncated data set,³ will be considered for comparison with relevant structural features of 4. Important crystallographic data of 1 and 4 are collected in Table II.

Compound 4 is, like 1, a three-dimensional coordination polymer whose octahedral $\text{Co}(\text{CN})_6$ units are continuously interlinked by practically planar Me_3E fragments. All the main-group metal atoms E become thus five-coordinate, the cyanide N atoms occupying throughout the axial tbp positions. According to Lehn's well-accepted description,²³

(22) See: (a) Shriver, D. F. *Struct. Bonding* 1966, 1, 32. (b) Bertrán, J. F.; Pascual, J. B.; Ruiz, E. R. *Spectrochim. Acta* 1990, 46A, 685.

Table III. Selected Bond Distances (Å) and Angles (deg) for 1 and 4

chain A			chain B			chain C		
distance/angle	Sn (1)	Pb (4)	distance/angle	Sn (1)	Pb (4)	distance/angle	Sn (1)	Pb (4)
E1-N2	2.36 (3)	2.52 (3)	E2-N5	2.20 (2)	2.54 (4)	E3-N1	2.28 (4)	2.52 (3)
E1-N4	2.23 (4)	2.52 (3)	E2-N6	2.34 (4)	2.52 (4)	E3-N3	2.53 (3)	2.46 (3)
C2-N2-E1	171 (2)	149 (3)	C5-N5-E2	159 (2)	145 (3)	C1-N1-E3	159 (4)	145 (2)
C4-N4-E1	172 (4)	154 (3)	C6-N6-E2	152 (4)	125 (3)	C3-N3-E3	134 (3)	140 (3)
N2-E1-N4	175 (1)	180 (1)	N5-E2-N6	170 (1)	177 (1)	N1-E3-N3	175 (2)	175 (1)

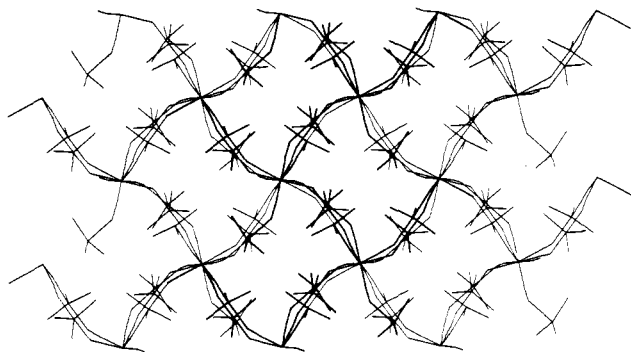
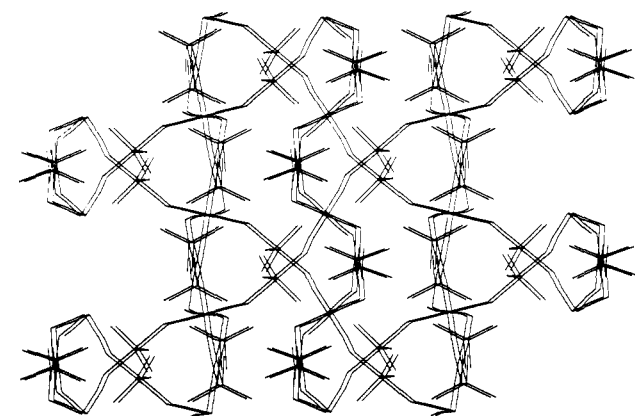


Figure 5. Lattice of 4; view along the main channels, i.e. [101].

Figure 6. Lattice of 4; viewed along *c*, [001] (see also Figure 2).

the supramolecular 3D architecture of 1 and 4 can be considered to be a result of "spontaneous self-assembly". While Figures 1 and 2 present the unit cells of 1 and 4 along with the atomic numbering schemes, graphs like those depicted in Figures 3–6 may offer a better insight into the construction of the lattice along the most dominant, parallel channels and perpendicular to them, respectively. The drawings of the structure of 1 appear virtually identical with those resulting from the earlier treatment of the X-ray data.³ Mainly owing to different C–N–E angles in 1 and 4 (average values: 1, 158°; 4, 143°), the structure of 4 appears to look more "collapsed", or more compact, as compared with that of 1 (vide infra).

Although the lattices of 1 and 4 are not superimposable and X-ray powder diagrams of 1⁴ and 4 bear no immediate resemblance, some common features become more clearly apparent after the reexamination of the structure of 1. Since those $[-\text{Co}-\text{C}\equiv\text{N}-\text{Sn}-\text{N}\equiv\text{C}-]_{\infty}$ chains of 1 initially thought³ to be strictly linear now turn out to be modestly bent as well (Table III), one consequence (e.g. of relevance for solid-state NMR spectroscopy) is the requirement to describe both lattices in terms of three

crystallographically nonequivalent, infinite chains A, B, and C. Interestingly, the close crystallographic similarity chain A: $[-\text{Co1}-\text{C2}-\text{N2}-\text{E1}-\text{N4}-\text{C4}-\text{Co2}-\text{C4}'-\text{N4}'-\text{E1}'-\text{N2}'-\text{C2}'-]_{\infty}$

chain B: $[-\text{Co2}-\text{C5}-\text{N5}-\text{E2}-\text{N6}-\text{C6}-\text{Co2}'-\text{C6}'-\text{N6}'-\text{E2}'-\text{N5}'-\text{C5}'-]_{\infty}$

chain C: $[-\text{Co1}-\text{C1}-\text{N1}-\text{E3}-\text{N3}-\text{C3}-\text{Co1}'-\text{C3}'-\text{N3}'-\text{E3}'-\text{N1}'-\text{C1}'-]_{\infty}$ (2)

of chains A and B of 1 is even reflected by an "accidental" degeneracy at room temperature of two Me_3Sn carbon-13 resonances (vide infra). All C–Co–C sections within each chain are practically linear. Some significant intrachain distances and bond angles, respectively, of 1 and 4 are collected in Table III. Interestingly, chain C of both compounds displays the most unsymmetrical bridge ($\text{N1}\cdots\text{E3}\cdots\text{N3}$) with respect to the N–E distances, while the corresponding bridges $\text{N2}\cdots\text{E1}\cdots\text{N4}$ and $\text{N5}\cdots\text{E2}\cdots\text{N6}$ of chains A and B turn out to be more symmetrical. The $\text{N1}\cdots\text{Sn3}\cdots\text{N3}$ bridge of 1 is reminiscent of the likewise very unsymmetrical $\text{O1}\cdots\text{Sn1}\cdots\text{N2}$ bridge within chain B of the recently described polymer $[(\text{Me}_3\text{Sn})_4\text{Fe}(\text{CN})_6\cdot 2\text{H}_2\text{O}\cdot \text{C}_4\text{H}_8\text{O}_2]_{\infty}$.²⁵ Chain A of this latter polymer displays N \cdots Sn \cdots N bridges whose adjacent C–N–Sn sequences compare well, in view of both the Sn–N distance and the C–N–Sn angles, with, e.g., the fragments C5–N5–Sn2, C6–N6–Sn2, and C1–N1–Sn3 of 1. The E atom of chains A (E = Sn and Pb) and C (E = Sn only) lie coplanar within the three methyl carbon atoms, while Sn2, Pb2, and Pb3 are located 0.10–0.13 Å above their $[\text{C}(\text{Me})_3]$ planes (i.e. closer to N6 and N3, respectively).

The (fixed) Pb–C(Me) distance of 4 (2.25 Å) lies close to the values of most of the so far investigated Me_3PbX systems, while the experimental Pb–N distances of 4 compare best with the value of the polymeric azide, $[\text{Me}_3\text{Pb}(\mu\text{-N}_3)]_{\infty}$ (2.58 Å).²⁶ The lattices of 1 and 4 display, moreover, several sites with interchain N \cdots N' distances ranging between 4 and 7 Å, e.g. in 4: N2 \cdots N4', 4.60 Å; N1 \cdots N3', 4.82 Å; N1 \cdots N6', 5.85 Å. Such relatively close-lying pairs of N atoms might in principle be capable of anchoring suitable Lewis acidic guests within the clefts between the two chains. Possibly, the still unknown crystal structures of the surprisingly stable, virtually anhydrous compounds $[(\text{Me}_3\text{E}')(\text{Me}_3\text{E})_3\text{M}(\text{CN})_6]_{\infty}$ (with E' = Sn and/or Pb, M = Fe, Ru, Os), whose E atoms appear (spectroscopically) to be all tbp-configured,⁸ might involve "excess" $\text{Me}_3\text{E}/\text{Me}_3\text{E}'$ cations accommodated between two potentially "chelating" N atoms inside the cavities.^{27,28}

(25) Adam, M.; Brimah, A. K.; Fischer, R. D.; Li, X.-F. *Inorg. Chem.* 1990, 29, 1595.

(26) (a) Allmann, R.; Waskowska, A.; Hohlfield, R.; Lorberth, J. *J. Organomet. Chem.* 1980, 198, 155. (b) The two Pb–N distances within each tbp-configured Me_3PbN_2 unit are practically identical.

(27) See also: Behrens, U.; Brimah, A. K.; Fischer, R. D. *J. Organomet. Chem.* 1991, 411, 325.

(28) Several organolead(IV) polymers of the type $[(\text{Me}_3\text{Pb})_4\text{M}(\text{CN})_6\cdot n\text{H}_2\text{O}]_{\infty}$ ($n = 0$ or 2) have likewise been prepared and subjected to crystallographic X-ray studies: Brimah, A. K.; Soliman, T. M.; Fischer, R. D. To be published.

(23) Garrett, T. M.; Koert, U.; Lehn, J.-M.; Rigault, A.; Meyer, D.; Fischer, J. *J. Chem. Soc., Chem. Commun.* 1990, 557. See also: Lehn, J.-M. *Angew. Chem.* 1988, 100, 91; *Angew. Chem., Int. Ed. Engl.* 1988, 27, 1121.

(24) Walker, N.; Stuart, D. *Acta Crystallogr.* 1983, A39, 158.

Table IV. Comparison of the "Formula Weight Volumes", V_{fw} , of Several Polymeric or Saltlike $[A_3M(CN)_6]_n$ Systems

$[A_3M(CN)_6]_n$ system	$V_{fw}(\text{exp})^a$ cm ³ /mol	$V_{fw}(\text{cub})^{a,b}$ cm ³ /mol	ref ^c
$[H_3Co(CN)_6]_n$	125	400	6b ^d
$K_3[Fe(CN)_6]$	180 ^e		29
$[Ag_3Co(CN)_6]_n$	185	628	7 ^e
$(NMe_4)_2Cs[Fe(CN)_6]$	305		30
$[(Me_3Pb)_3Co(CN)_6]_n$	435	810	this paper
$[(Me_3Sn)_3Co(CN)_6]_n$	460	730	this paper
$[(Cp_2Co)(Me_3Sn)_3Fe(CN)_6]_n^{f,g}$	550	730	10

^a $V_{fw} = M_r/D_c$. ^b $V_{fw}(\text{cub})$ refers to the still hypothetical super-Prussian-blue (SPB) like network (see text). ^c Source of all X-ray densities, D_c , and interatomic distances of relevance, respectively. ^d $(N\cdots H)_{av} = 1.35$ Å. ^e $(Ag-N) = 2.06$ Å. ^f With Cp_2Co^+ as guest cation ($Cp = \eta^5-C_5H_5$). ^g Ignoring any blow-up of the host network; $V_{fw}(\text{exp})$ of the species with (methylviologen)²⁺ as guest and Ru instead of Fe^9 would amount to 495 cm³/mol. ^h Based on pycnometric density measurements, V_{fw} of $[(Et_4N)_3Fe(CN)_6]$, amounts to 204 cm³/mol.

Attempt To Quantify the Internal Cavity Volume

The obviously more collapsed appearance of the lattice of 4 relative to that of 1 (vide supra) is also reflected when the "formula weight volumes", $V_{fw} = M_r/D_c$ (M_r = formula weight; D_c = calculated density), of the two polymeric $A_3Co(CN)_6$ congeners 1 and 4 are compared (Table IV). Although the considerably longer Pb-N distances in 4 (average 2.50 Å; average Sn-N distance in 1 2.32 Å) are expected to make the V_{fw} of 4 even larger than the V_{fw} of 1, a significant reduction of the V_{fw} of 4 results owing to the still more pronounced average deviation of the angle C-N-Pb from 180° (vide supra). The rather low experimental V_{fw} values of the two purely inorganic polymers $[A_3Co(CN)_6]_n$ ($A = Ag, H$) compare best with the value of the genuine salt $K_3[Fe(CN)_6]$, but replacement of the three K^+ ions by two notably larger Me_4N^+ ions and one Cs^+ ion is seen to lead (Table IV) to an increase in V_{fw} by ca. 65%. Since the total net space demand of three of these latter cations is likely to even exceed that of three Me_3Sn^+ ions, the likewise drastic increase of V_{fw} from $(Me_4N)_2Cs[Fe(CN)_6]$ to $[(Me_3E)_3Co(CN)_6]_n$ by ca. 43 and 51%, respectively (Table IV), should be due to the unique architecture of the lattices of 1 and 4 in which the Me_3E groups function as spatially well-oriented spacers. Actually, an uptake of $(C_5H_5)_2Co^+$ guest cations by the negatively charged host network $[(Me_3Sn)_3Fe(CN)_6]_n^{10}$ leads only to a moderate further increase of V_{fw} (relative to V_{fw} of 1), in view of an experimental V_{fw} value of ca. 123 cm³/mol for the ferrocene molecule.^{31,32}

Obviously, the presence of organic groups in the organometallic bridging units A of 1 and 4 is responsible for the different packing of their $Co(CN)_6$ octahedra as compared with that in, e.g., $[H_3Co(CN)_6]_n$.^{6b} Groups R of higher steric congestion than CH_3 like Bu^n or $\eta^5-C_5H_5$ (with $E = U^{1,3}$) could in principle cause a further blow-up of the lattice toward the ultimately cubic "super-Prussian-blue" (SPB) arrangement with exclusively linear $[-M-C\equiv N \rightarrow A \leftarrow N\equiv C-]_n$ chains.³ The theoretical $V_{fw}(\text{cub})$ values of some polymers adopting the still hypothetical SPB net-

Table V. Comparison of the Numbers of Crystallographically Nonidentical Atoms with the Respective Numbers of Observable NMR Resonances

	C(CH ₃)	C(CN)	N	Sn/Pb	Co
XRS	1, 4	9	6	3	2
NMR	1	2 (3 ^c)	b	3	1
NMR	4	3 (3 ^c)	b	1 ^a	2

^a Preliminary result (S/N poor). ^b Not determined as the spectra are complex. ^c Between -20 and -60 °C.

Table VI. Collection of NMR Data for 1 and 4

	$[(Me_3Sn)_3Co(CN)_6]_n$ (1)		$[(Me_3Pb)_3Co(CN)_6]_n$ (4)	
	δ , ppm	$I_{rel}/\text{ass'tmt}$	δ , ppm	$I_{rel}/\text{ass'tmt}$
¹³ C	-0.5 ^f (570) ^b	1/CH ₃	16 (414)	1/CH ₃
	0.8 ^g (550) ^b	2/CH ₃	17 (375) ^c	1/CH ₃
¹¹⁹ Sn	ca. 132	CN	18 (373) ^c	1/CH ₃
	-88	2	ca. 135	CN
²⁰⁷ Pb	-118	1	172	2
	-116	1	78	1
¹⁵ N	-119	1		
	-123	1	-124	
⁵⁹ Co	-244 ^d (558) ^e		-157 (800) ^e	

^a Data taken from ref 11. ^b Value in parentheses: $^1J(^{119}Sn-^{13}C)$ in hertz. ^c Value in parentheses: $^1J(^{207}Pb-^{13}C)$ in hertz. ^d The value $\delta(^{59}Co) = -225$ ppm has been reported earlier.³ Our results for $[(Et_3Sn)_3Co(CN)_6]_n$ and $[(Bu^t)_3Sn)_3Co(CN)_6]_n$ are $\delta(^{59}Co) = -234$ and $+206$ ppm. ^e Value in parentheses: line width in hertz. ^f Shifts to -0.80 ppm at -60 °C. ^g Splits into singlets at 0.44 and 0.73 ppm at -60 °C.

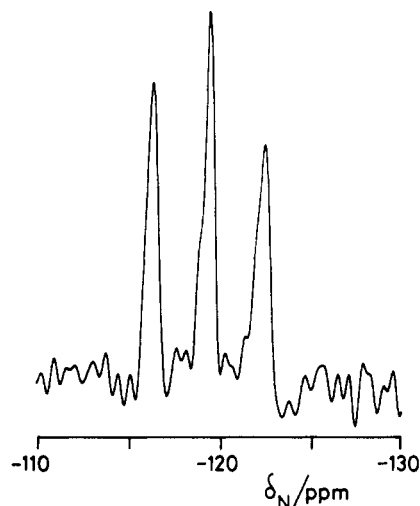


Figure 7. Nitrogen-15 CP MAS NMR spectrum at 30.4 MHz for $[(Me_3Sn)_3Co(CN)_6]_n$. The existence of three cyanide environments is demonstrated. Spectrometer operating conditions: contact time 5 ms, relaxation delay 2 s, number of transients 38 300, spin rate 4820 Hz.

work are likewise given in Table IV. The large differences of $V_{fw}(\text{cub})$ and $V_{fw}(\text{exp})$ suggest that the corresponding SPB-configured modifications should, in the absence of any void-supporting organic groups R or space-filling guests G^+ , be thermodynamically rather unfavorable.^{3a}

Solid-State NMR Studies

The crystal structures of 1 and 4 described above provide a particularly challenging starting point for an in-depth evaluation of the CP MAS solid-state NMR spectra of the majority of NMR-suitable nuclei available in 1 and 4. Fortunately, the numerous methyl protons of the organometallic units help to strongly improve, via cross polarization, the observation of, e.g., ¹¹⁹Sn, ²⁰⁷Pb, and even ¹⁵N resonance signals. In the following discussion some

(29) Fletcher, S. R.; Gibb, T. C. *J. Chem. Soc., Dalton Trans.* 1977, 309.

(30) Babel, D. *Z. Naturforsch.* 1982, 37B, 1534.

(31) The V_{fw} value of Cp_2Fe was determined using crystallographic details from: (a) Eiland, P. F.; Pepinsky, R. *J. Am. Chem. Soc.* 1952, 74, 4971. (b) Seiler, P.; Dunitz, J. D. *Acta Crystallogr.* 1979, B35, 2020. (c) See also: Edward, J. T. *J. Chem. Educ.* 1970, 47, 261.

(32) Actually, the pure host lattice is no longer isostructural with that of 1.¹⁰

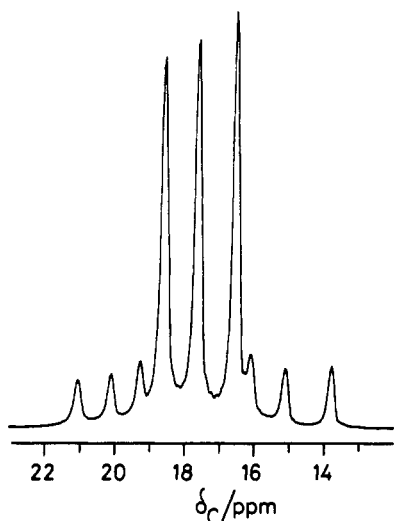


Figure 8. Methyl region of the 75.4-MHz ^{13}C CP MAS NMR spectrum of $[(\text{Me}_3\text{Pb})_3\text{Co}(\text{CN})_6]_\infty$. The satellite peaks arising from ^{207}Pb , ^{13}C coupling may be clearly seen. Spectrometer operating conditions: contact time 10 ms, relaxation delay 1 s, number of transients 53 540, spin rate 4140 Hz.

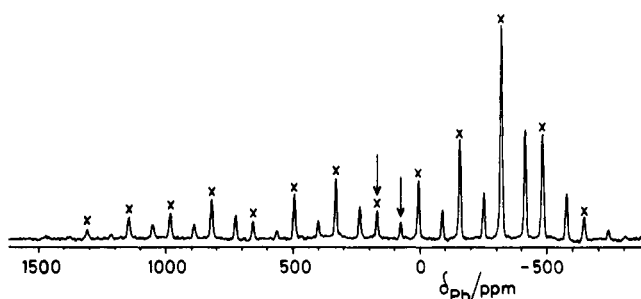


Figure 9. Lead-207 CP MAS NMR spectrum at 62.7 MHz for $[(\text{Me}_3\text{Pb})_3\text{Co}(\text{CN})_6]_\infty$, obtained using a 5-mm-o.d. rotor. The two center bands are marked by vertical arrows, and the spinning sideband manifold for the high-frequency resonance is indicated by asterisks. Spectrometer operating conditions: contact time 5 ms, relaxation delay 2 s, number of transients 29 520, spin rate 10 360 Hz.

reported¹¹ NMR results for 1 are included. In Table V the numbers of crystallographically nonequivalent C, N, Co, Sn, and Pb atoms of 1 and 4 are compared with the corresponding numbers of actually observed resonance lines. The full experimental NMR data obtained for the nuclei: ^{13}C , ^{15}N , ^{59}Co , ^{119}Sn , and ^{207}Pb are listed in Table VI. Figure 7 shows the ^{15}N spectrum of 1 (not previously reported), while Figures 8 and 9 illustrate the ^{13}C and ^{207}Pb spectra of 4, respectively.

The appearance of (at least between -20 and -60 °C) no more than three sharp, symmetric methyl carbon resonances for 1 and 4, respectively, may conceivably be due to rapid (on the NMR time scale) rotation of the Me_3E fragments about their 3-fold N-E-N axes. Although such a process seems intrinsically unlikely, preliminary low-temperature ^{13}C experiments (down to -60 °C) on $[(\text{Me}_3\text{Sn})_4\text{Os}(\text{CN})_6]_\infty$ showed typical chemical-exchange effects,^{33b} with an increased number of methyl carbon peaks being observed below -40 °C. However, similar

experiments revealed no significant changes in the ^{13}C spectrum of 1 or 4. The X-ray structures of both 1 and 4 imply individual fixed positions for all nine methyl carbon atoms although several methyl C atoms of 4 appear to be notably disordered (cf. Experimental Section). In contrast, the ^{13}C CP MAS NMR spectrum of solid, and most probably polymeric, Me_3PbOMe displays three well-separated PbMe carbon resonances, while the corresponding ^{207}Pb NMR spectrum indicates only a single lead site.³⁵

Interestingly, from the CP MAS ^{13}C NMR spectra of 1 and 4 as many different values for the coupling parameters $^1J(\text{E}-^{13}\text{C})$ as for the $\delta(^{13}\text{C},\text{Me})$ data are evaluated. Not only the experimental $^1J(^{119}\text{Sn}-^{13}\text{C})$ values¹¹ but also the coupling parameters $^1J(^{207}\text{Pb}-^{13}\text{C})$ of 373–414 Hz compare well with those for some examples of tbp-configured adducts $\text{Me}_3\text{PbX}\cdot\text{L}$ studied in solution (e.g. for X = Cl and L = pyridine, $J = 378$ Hz, and for X = CH_3COO and L = H_2O , $J = 422$ Hz).^{35,36} On the other hand, Me_3PbX derivatives with essentially tetracoordinate lead atoms display notably smaller J values (253–318 Hz).³⁵ In accordance with the crystallographically confirmed pentacoordination of the lead atoms, the chemical shifts for the two ^{207}Pb resonances of 4 compare well with that of solid Me_3PbOMe (103.8 ppm)³⁴ but appear at notably lower frequency than those of several probably tbp-configured $\text{R}_3\text{Pb}(\text{CH}_3\text{COO})$ derivatives (R = alkyl) which have been reported to lie between 317 and 428 ppm. On the other hand, tetracoordinate Me_3PbR systems with less electronegative ligands R (e.g. Eg, Prⁱ, Buⁿ, etc.) display $\delta(^{207}\text{Pb})$ values even closer to zero than solid Me_3PbOMe .³⁵ Some recent examples of non-tbp-configured $\text{Me}_2\text{R}_2\text{Pb}^{\text{IV}}$ derivatives with virtually likewise pentacoordinate lead atoms have been reported³⁴ to show $\delta(^{207}\text{Pb})$ values at very high frequencies (ca. 670 ppm).

It is very surprising to find that for both 1 and 4 NMR detects fewer inequivalences than predicted by XRD results for all four accessible nuclei. Because the XRD time scale is effectively the exposure time, one would normally expect this technique to indicate more inequivalences than NMR if molecular motions are in question. Moreover, the chemical shifts of the metal atoms are known to be very sensitive to minor variations in chemical structure. We have no rational explanation of the observed discrepancies at present, though one should note that in general, resolution limitations restrict NMR spectroscopy to estimating the *minimum* number of atoms of a given type in the asymmetric unit.

For the fine details of the $\delta(^{119}\text{Sn})$ and $\delta(^{207}\text{Pb})$ values of E atoms in crystallographically different environments, distinct structural parameters such as the N-E distance and/or the C-N-E angle might be of major relevance. Thus, the (C1N1) $\text{Me}_3\text{Sn}3(\text{N}3\text{C}3)$ unit of chain C in 1 differs most significantly from the two other $\text{Me}_3\text{Sn}(\text{NC})_2$ units in view of both its rather unsymmetrical N1-Sn3-N3 arrangement and the Sn-N-C angles (vide supra, Table III). The observation of only two, instead of three, ^{119}Sn resonances would then imply that the structural parameters of the two less distorted $\text{Me}_3\text{Sn}(\text{NC})_2$ units of chains A and B differ too insignificantly from each other to give rise to two separate ^{119}Sn resonances. This ad hoc explanation contrasts with the one given recently,¹¹ when the more intense signal was "intuitively" assigned to the "strictly linear" chains, and the other one to the (more

(33) (a) Probably for this reason, our attempts to also arrive at polymers like $[(\text{Me}_3\text{Sn})_2\text{Zn}(\text{CN})_4] = [\text{Zn}(\mu\text{-CNSnMe}_3\text{NC})_2]_\infty$ have so far remained unsuccessful.^{33b} (b) Apperley, D. C.; Davies, N. A.; Harris, R. K.; Eller, S.; Schwarz, P. To be published in *J. Chem. Soc., Chem. Commun.*

(34) Wrackmeyer, B.; Horchler, K.; Sebald, A.; Merwin, L. H. *Magn. Reson. Chem.* 1990, 28, 465. Apparently, the coupling parameters $^1J(^{13}\text{C}-^{207}\text{Pb})$ of the three PbC(Me) resonances of solid Me_3PbOMe ($\delta(^{13}\text{C})$: 19.9, 18.2, 15.0 ppm) could not be determined.

(35) Mitchell, T. N.; Gmehling, J.; Huber, F. *J. Chem. Soc., Dalton Trans.* 1978, 960.

(36) For the most recent survey on relevant ^{207}Pb NMR results see: Wrackmeyer, B.; Horchler, K. *Annu. Rep. NMR Spectrosc.* 1990, 22, 249.

Table VII. Tentative Assignment of Observed ^{119}Sn and ^{207}Pb Resonances to Symmetrical and Unsymmetrical N...E...N Bridges

sample	$\delta(\text{X})$, ppm; X = ^{119}Sn or ^{207}Pb	
	distorted ^a	almost undistorted ^a
	N-X...N' unit	N-X-N' unit
1 ¹¹	-118 (1)	-88 (2)
4	78 (1)	172 (2)
6 ²⁵	-136 (1)	-73 (1)
7 ¹¹		-75

^a With respect to N-X bond length.

abundant) nonlinear chains.

The same argument would suggest for 4 that its less intense ^{207}Pb resonance should be ascribed either to chain C because of the relatively unsymmetrical N1-Pb3-N3 bridge (in view of the Pb-N distances) or to chain B owing to its two quite different Pb-N-C angles (Table III). Again, it seems that only the major structural nonequivalence leads to individual $\delta(^{207}\text{Pb})$ values, although the magnitude of the separation of the two observed Pb resonances of 4 (94 ppm!) is quite large. Interestingly, the unsymmetrical Me_3PbO_2 unit of the polymeric acetate with two notably different Pb-O distances³⁷ displays a more positive $\delta(^{207}\text{Pb})$ value³⁵ than the probably more symmetrical^{26b} Me_3PbO_2 unit in solid Me_3PbOMe .³⁴ The less intense resonance of the nucleus of E appears for both 1 and 4 at a frequency lower than that of the second, more intense signal (vide infra); also these latter features contrast with the earlier assignment.¹¹

The three almost equally intense ^{15}N resonances of 1 (Table V and Figure 7), which lie close to each other, are likely to represent cyanide N atoms whose C-N-Sn angles and/or N-Sn distances fall into distinct ranges. The data of Table IV suggest that the six crystallographically different N atoms might be divided into three subgroups, namely (N2, N4), (N1, N5, N6), and (N3). Interestingly, the longest Sn-N bond (Sn3-N3) is combined with the most acute C-N-Sn angle. However, for the shortest Sn-N bond (Sn2-N5) the reverse is not quite true. Owing to the considerable technical problems accompanying practical solid-state ^{15}N NMR work on samples like 1 and 4 devoid of any ^{15}N enrichment, this rather promising branch of NMR spectroscopy will deserve a reexamination with ^{15}N -enriched samples. The ^{15}N NMR spectrum of 4 shows, for the time being, a still unsatisfactory signal to noise ratio and only one resonance at δ -124 ppm. Similarly, the usually rather complex, albeit weak cyanide ^{13}C resonances appear worth being studied in more detail as soon as ^{13}C - and ^{15}N -enriched samples become available. The main cyanide ^{13}C center bands of 1 and 4 appear around 135 ppm. Somewhat unexpectedly, the ^{13}C resonance of the nonbridging CN groups in $[(\text{Et}_3\text{N})_3\text{Co}(\text{CN})_6]$ does not lie significantly apart (Table VIII).

Solid-state ^{59}Co NMR spectroscopy does not discriminate between the two crystallographically nonequivalent Co atoms Co1 and Co2 of 1 and 4 although the ^{59}Co nucleus is known to be particularly sensitive even to weak variations in its chemical surroundings. Thus, the chemical shift $\delta(^{59}\text{Co})$ of the dissolved complex $[\text{Co}(\text{CN})_6]^{3-}$ anion is known to vary notably with the nature of its counterion and/or of the solvent. While organic cations R_4N^+ (R = alkyl) tend to shift the resonance of {crown ether- K^+ } $[\text{Co}(\text{CN})_6]$ solutions in Me_2SO to higher frequencies,³⁸ the reverse takes place when water or proton acids are

Table VIII. Solid-State NMR Data for $[\text{A}_3\text{Co}(\text{CN})_6]$ with A = Bu^n_3Sn , H, Et_3N

A	^{13}C	$I_{\text{rel}}/\text{ass}^{\text{mt}}$	^{119}Sn	^{15}N	^{59}Co
Bu^n_3Sn	14.8	2/Me	-42	-118 ^c	206 (2500) ^e
	14.5	1			
	20.0 (464) ^b	2/ $\text{CH}_2(\text{Sn})$			
	18.4 (468) ^b	1			
	28.2	CH_2			
	27.5				
	27.4				
ca. 130	CN				
H	118			-134	-258 (1645) ^e
Et_3N	9.2 ^a	1/Me		-89.8	208 (1039) ^e
	8.3 ^a	3		-311 ^d	
	52.7	CH_2			
	ca. 132	CN			

^a The peak at 9.2 ppm is much sharper than that at 8.3 ppm.

^b Values in parentheses are $|^1J_{\text{SnC}}|$ in hertz, with ^{119}Sn and ^{117}Sn not differentiated. ^c $|^1J_{\text{Sn}^{15}\text{N}}| = 147$ Hz. ^d Et_3N resonance. ^e Line width in hertz.

added.³⁹ The data of Tables VI and VIII indicate that likewise $\delta(^{59}\text{Co})$ of solid $\text{A}_3\text{Co}(\text{CN})_6$ samples considered is scattered over a range of 500 ppm. Variation of A influences $\delta(^{59}\text{Co})$ in the sequence $\text{Et}_4\text{N} \sim \text{Bu}^n_3\text{Sn} > \text{Me}_3\text{Pb} > \text{Et}_3\text{Sn} \sim \text{Me}_3\text{Sn} > \text{H}$. Only one symmetrical center band resonance surrounded regularly by a wide spread of weaker spinning side bands is usually recorded.

Table VIII gives NMR data for three compounds of the type $\text{A}_3\text{Co}(\text{CN})_6$ not presented previously. The cases chosen are A = H (probably strongly bridging), A = Bu^n_3Sn (probably moderately bridging), and A = NEt_4 (non-bridging^{6b}). The compound with A = Bu^n_3Sn gives a high-quality ^{15}N spectrum which makes it clear that all the CN groups are equivalent on the NMR time scale, as for the case with 7, A = Et_3Sn (which gives a single ^{15}N line at $\delta(^{15}\text{N}) = -120$ ppm). The value of $|^1J_{\text{Sn}^{15}\text{N}}| = 147$ Hz, obtained from the ^{15}N resonance, is reasonably consistent with our deductions from the fine structure of the ^{119}Sn resonance of A = Et_3Sn , which yield $|^1J_{\text{Sn}^{14}\text{N}}| = 125$ Hz. The cyanide carbon resonance for A = Bu^n_3Sn shows no fine structure, though the envelope of its center band is similar to that for A = Et_3Sn . The single ^{119}Sn center band is also consistent¹¹ with the result for A = Et_3Sn , making it highly likely that the crystal structures of these two compounds are analogous. Quite unexpectedly, however, the ^{59}Co shift of the sample with A = Bu^n_3Sn differs strongly from, e.g., that with A = Et_3Sn in 7. The actual difference in $\delta(^{59}\text{Co})$ is larger than that observed for dissolved samples with A = Et_3N and Bu^n_4N , respectively.³⁸ The alkyl ^{13}C features differ also in that the spectrum for A = Bu^n_3Sn suggests strongly that one of the alkyl groups is in a distinctly different environment from the other two (in contrast to the case for A = Et_3Sn). This finding possibly indicates that, unlike the smaller R_3Sn fragments, Bu^n_3Sn may no longer rotate freely about its N-Sn-N axis.

The methyl region of the ^{13}C spectrum for A = Et_3N also shows significant inequivalences, while the ^{15}N spectrum displays a single peak for the six nonbridging CN nitrogen along with another signal in the region expected ($\delta(^{15}\text{N}) = -311$ ppm) for the NEt_4 group. The former ^{15}N shift appears at a frequency higher than the $\delta(^{15}\text{N})$ values of all $[\text{A}_3\text{Co}(\text{CN})_6]$ systems with A = R_3E (E = Sn or Pb), whose frequencies exceed, in turn, that of $[\text{H}_3\text{Co}(\text{CN})_6]^\infty$. Solid-state ^{15}N NMR data of two other samples with strong $\text{M}-\text{C}\equiv\text{N}\cdots\text{H}\cdots\text{N}\equiv\text{C}-\text{M}'$ bridges have most recently been published⁴⁰ along with the ^{15}N shift of a complex involving

(37) Sheldrick, G. M.; Taylor, R. *Acta Crystallogr.* 1975, B31, 2740.
 (38) (a) Laszlo, P.; Stockis, A. *J. Am. Chem. Soc.* 1980, 102, 7818. (b) Delville, A.; Laszlo, P.; Stockis, A. *J. Am. Chem. Soc.* 1981, 103, 5991.

(39) Eaton, D. R.; Rogerson, C. V.; Sandercock, A. C. *J. Phys. Chem.* 1982, 86, 1365.

one CNH ligand whose ^{15}N shift is still more negative than those with hydrogen bridges. Accordingly, $\delta(^{15}\text{N})$ of a terminal cyano ligand is less negative than $\delta(^{15}\text{N})$ of two R_3E - and H-bridged CN groups, respectively, while the ^{15}N shift of the terminal CNH ligand is even more negative than that of a $\text{M}-\text{CN}\cdots\text{H}\cdots\text{NC}-\text{M}'$ fragment.⁴⁰

Concluding Remarks

The two coordination polymers 1 and 4 represent the first well-established examples of guest-free cyanide-bridged 3D networks $[(\text{R}_3\text{E})_n\text{M}(\text{CN})_{2n}]_\infty$ whose transition-metal-bonded cyanide ligands are linked pairwise by efficient Me_3M spacer groups ($\text{E} = \text{Sn}$ or Pb). The results of single-crystal X-ray diffraction studies, systematic formula-weight-volume considerations and successful attempts to introduce large cations into corresponding lattices demonstrate unequivocally that the 3D networks of 1 and 4 involve unusually wide internal cavities. Nevertheless, notable deviations of the C-N-E angles from 180° indicate that, most probably for thermodynamic reasons, the maximal cavity volume of an ideal "super-Prussian-blue" (SPB) structure is not reached. Interesting consequence of these findings will be the subject of subsequent studies on related polymers, $[(\text{R}_3\text{E})_n\text{M}(\text{CN})_{2n}]_\infty$, with $n = 2$ (i.e. tetrahedral metal coordination) and $n = 4$, respectively.

In some contrast to a previous view,¹¹ the room-temperature ^{119}Sn and ^{207}Pb NMR spectra of 1 and 4 appear in general incapable of reflecting *all* crystallographically different $\text{Me}_3\text{E}(\text{NC})_2$ units, and seem thus to differentiate only grossly between "less and more strongly asymmetric" fragments. Both the cyanide ^{15}N and methyl ^{13}C NMR spectra may allow more subtle distinctions provided that satisfactorily intense resonances can be observed. Since the $\text{N1Me}_3\text{Sn3N3}$ unit of chain C of 1 is structurally similar to the $\text{N2Me}_3\text{Sn1O1}$ unit in chain B of the polymer $[(\text{Me}_3\text{Sn})_4\text{Fe}(\text{CN})_6\cdot 2\text{H}_2\text{O}\cdot \text{C}_4\text{H}_8\text{O}_2]_\infty$ (6)²⁵ (vide supra), the alternative correlation of their ^{119}Sn or ^{207}Pb resonances according to Table VII might be suggested.

The ethyl homologue of 1, $[(\text{Et}_3\text{Sn})_3\text{Co}(\text{CN})_6]_\infty$ (7), which may be expected to exhibit a somewhat larger formula weight volume, V_{fw} , than 1 owing to the slightly larger spatial demand of its alkyl groups (vide supra) has already been shown by solid-state ^{13}C and ^{119}Sn NMR spectroscopy to be built up of a single type of $[-\text{Co}-\text{C}\equiv\text{N}-\text{Sn}-\text{N}\equiv\text{C}-]_\infty$ chain, although a cubic crystal structure must be ruled out.¹¹ This view appears to be nicely confirmed now by the observation of only one sharp ^{15}N resonance at -120 ppm, and likewise one symmetrical ^{59}Co resonance whose δ value almost coincides with that of 1 (Table VI), presumably by accident. Since 7, as well as the 1D polymer $[(\text{Me}_3\text{Sn})\text{Au}(\text{CN})_2]_\infty$ ($\delta(^{119}\text{Sn}) = -64$ ppm¹¹), is unlikely to contain (exclusively) notably *unsymmetrical* $\text{C}_3\text{Sn}(\text{NC})_2$ units, attention must still be paid to the somewhat paradoxical view that $\text{C}_3\text{E}(\text{NC})_2$ units with a most perfect *tbp* arrangement display less negative $\delta(^{119}\text{Sn})$ values than considerably distorted ones. It should be noted that the ^{119}Sn NMR spectra of *dissolved* *tbp*-configured samples tend to display a shift of $\delta(^{119}\text{Sn})$ toward higher frequencies concomitantly with an increasing distortion along the trigonal axis.⁴¹ However, solution spectra may be influenced by sufficiently rapid (on the NMR time scale) *tbp*/ ψ - T_d interconversions whose activity is hard to take account of.

Table IX. Positional Parameters with Standard Deviations and Thermal Parameters for 4

atom	x/a	y/b	z/c	$U_{\text{eq}}, \text{\AA}^2$
Pb1	0.7868 (1)	0.8250 (1)	0.4866 (1)	0.098 (1)
Pb2	1.1190 (1)	0.7317 (1)	0.7826 (1)	0.102 (1)
Pb3	0.4396 (1)	0.6415 (1)	0.6518 (1)	0.089 (1)
Co1	0.5000	1.0000	0.5000	0.063 (3)
Co2	1.0000	0.5000	0.5000	0.075 (3)
N1	0.467 (2)	0.769 (2)	0.528 (2)	0.10 (1)
N2	0.665 (2)	0.951 (2)	0.464 (3)	0.12 (1)
N3	0.578 (2)	1.024 (3)	0.718 (2)	0.12 (1)
N4	0.909 (2)	0.699 (2)	0.509 (2)	0.11 (1)
N5	1.102 (2)	0.610 (3)	0.385 (3)	0.14 (2)
N6	1.129 (2)	0.570 (3)	0.684 (2)	0.16 (2)
C1	0.480 (1)	0.855 (2)	0.513 (2)	0.06 (1)
C2	0.599 (2)	0.970 (3)	0.475 (3)	0.08 (1)
C3	0.548 (2)	1.007 (2)	0.637 (2)	0.08 (1)
C4	0.939 (2)	0.618 (2)	0.505 (3)	0.09 (1)
C5	1.057 (3)	0.566 (3)	0.423 (3)	0.12 (3)
C6	1.080 (2)	0.545 (3)	0.614 (2)	0.10 (2)
C7	0.750 (5)	0.818 (7)	0.324 (4)	0.33 (4)
C8	0.730 (6)	0.709 (7)	0.571 (4)	0.53 (7)
C9	0.882 (4)	0.943 (5)	0.565 (4)	0.32 (4)
C10	1.240 (1)	0.675 (3)	0.883 (2)	0.12 (1)
C11	0.997 (1)	0.665 (3)	0.802 (3)	0.15 (2)
C12	1.131 (3)	0.831 (4)	0.656 (2)	0.19 (3)
C13	0.565 (2)	0.560 (4)	0.672 (5)	0.26 (4)
C14	0.323 (2)	0.568 (4)	0.556 (3)	0.19 (3)
C15	0.430 (5)	0.785 (2)	0.740 (3)	0.28 (4)

Experimental Section

The purely inorganic samples $[\text{A}_3\text{M}(\text{CN})_6]$ with $\text{A} = \text{H}, \text{Ag},$ and NEt_4 ($\text{M} = \text{Co}$ or Fe) were prepared following published procedures.⁴²⁻⁴⁴ The earlier reported organometallic polymers $[\text{A}_3\text{Co}(\text{CN})_6]_\infty$ with $\text{A} = \text{Me}_3\text{Sn}, \text{Et}_3\text{Sn},$ and Bu_3Sn were obtained according to refs 1, 3, 8, and 11. The title compound 4 was precipitated by uniting solutions of 0.43 g (1.5 mmol) of Me_3PbCl and 0.17 g (0.5 mmol) of $\text{K}_3[\text{Co}(\text{CN})_6]$ in 50 and 40 mL of H_2O , respectively. After filtration, washing with a little cold H_2O , and short drying (ca. 60°C), 0.4 g of pure 4 (yield 83.2%) were obtained. Compound 5 had to be precipitated under exclusion of daylight, starting from solutions of 0.43 g (1.5 mmol) of Me_3PbCl in 50 mL of H_2O and 0.16 g (0.5 mmol) of $\text{K}_3[\text{Fe}(\text{CN})_6]$ in 35 mL of H_2O , respectively (yield 0.39 g = 81%). Elemental anal. calcd for $\text{C}_{15}\text{H}_{27}\text{N}_6\text{MPb}_3$ ($\text{M} = \text{Co}/\text{Fe}$): C 18.54/18.58, H, 2.78/2.79; N, 8.65/8.67; M, 6.06/5.78; Pb, 63.95/64.18. Found: C, 18.29/18.58; H, 2.90/3.02; N, 8.46/8.34; M, 5.25/5.68; Pb, 64.68/64.22. Infrared spectroscopic measurements were carried out on the Perkin-Elmer instruments 325, 577, and FT-IR-1720, respectively, and Raman spectra on the Ramanov U-1000 spectrometer of Jobin Yvon. The Johnson Matthey instrument MSB-MK I was used to determine magnetic susceptibilities at room temperature, and the Philips powder diffractometer PW 1050 (Cu $K\alpha$, Ni filter) to carry out Debye Scherrer X-ray diffraction studies.

White, needle-shaped single crystals of 4 were obtained within 2 days from a clear aqueous solution (80 mL) of 0.22 g (0.75 mmol) Me_3PbCl to which a solution of 0.09 g (0.25 mmol) $\text{K}_3[\text{Co}(\text{CN})_6]$ in 60 mL of H_2O had been added dropwise without stirring. Crystal data of relevance are given in Table II. The intensities of a total of 3883 reflections were measured by the $\omega/2\theta$ method of $2\theta_{\text{max}} = 47.5^\circ$. These were reduced and averaged to yield 3635 unique reflections, of which 1598 were judged observed ($F_o > \sigma(F_o)$). An empirical absorption correction (DIFABS²⁴) was applied. Final refinement (by full-matrix methods, SHELX-76⁴⁵) adopting 214 parameters and a weighting scheme of the form $w = (\sigma_F^2 + 0.0003F^2)^{-1}$ led to $R = 0.060$ and $R_w = 0.059$. All non-hydrogen atoms were refined anisotropically except the methyl C atoms C7, C8, and C9 (C atoms at Pb1). Pb-C lengths were fixed to

(42) Bär, E.; Fuchs, J.; Rieger, D.; Aguilar-Parrilla, F.; Limbach, H.-H.; Fehlhammer, W. P. *Angew. Chem.* 1991, 103, 88; *Angew. Chem., Int. Ed. Engl.* 1991, 30, 88.

(43) Ludl, A.; Güdel, H. U.; Dvorak, V. *Helv. Chim. Acta* 1967, 19, 2035.

(44) Alexander, J. J.; Gray, H. B. *J. Am. Chem. Soc.* 1968, 90, 4260.

(45) Sheldrick, G. M. SHELX-76, Programmes for Crystal Structure Determination. University of Cambridge, England, 1976.

(40) Bär, E.; Fuchs, J.; Rieger, D.; Aguilar-Parrilla, F.; Limbach, H.-H.; Fehlhammer, W. P. *Angew. Chem.* 1991, 103, 88; *Angew. Chem., Int. Ed. Engl.* 1991, 30, 88.

(41) Johnson, S. E.; Polborn, K.; Nöth, H. *Inorg. Chem.* 1991, 30, 1410.

2.25 Å; C–N lengths, to 1.15 Å. Some methyl C atoms, especially those at Pb1, display very high thermal parameters, indicating some disorder in these groups. Hydrogen atoms were not included in the calculations. A final difference Fourier map had a highest peak of $+1.7 \text{ e } \text{Å}^{-3}$ (located 1.13 Å from the Pb1 atom) and its lowest valley at $-0.98 \text{ e } \text{Å}^{-3}$. Table IX gives the atomic positions; further details including also anisotropic parameters and $|F_o|$ and $|F_c|$ values as well as an ORTEP plot of the asymmetric unit are included in the supplementary material.

The ^{15}N , ^{13}C , ^{59}Co , ^{119}Sn , and ^{207}Pb solid-state NMR spectra were obtained at 30.4, 75.4, 71.2, 111.9, and 62.7 MHz, respectively, using a Varian VXR 300 spectrometer in the cross-polarization mode (except for ^{59}Co) with Doty Scientific probes at ambient temperature (ca. 23 °C). For the lighter elements and for ^{59}Co 7-mm-o.d. rotors were employed, with typical MAS speeds in the range 4–5 kHz, whereas for ^{119}Sn and ^{207}Pb 5-mm-o.d. rotors with MAS rates of 10–13 kHz were generally used. For the cross-polarization experiments contact times in the range 1–10 ms and relaxation delays of 1–2 s were found to be appropriate. In general, many transients (10 000–60 000) were acquired for each spectrum, though for ^{13}C this was only necessary to obtain good sensitivity for the cyanide carbon signals. Center bands for ^{119}Sn and ^{207}Pb were determined by recording spectra at two different spinning speeds. For ^{59}Co spectra, 22 ° pulse angles with 0.5-s relaxation delays were used, and only 200–400 transients were required to get excellent S/N ratios. Chemical shifts are reported with the high-frequency-positive convention, in ppm with respect to the signals for solid NH_4NO_3 (nitrate line), SiMe_4 , $\text{K}_3[\text{Co}(\text{CN})_6]_{\text{aq}}$ (0.26 M), SnMe_4 , and PbMe_4 for ^{15}N , ^{13}C , ^{59}Co , ^{119}Sn , and ^{207}Pb , respectively. Typical line widths are ca. 20 Hz (^{15}N and ^{13}C), 300–2500 Hz (^{59}Co), ca. 250 Hz (^{119}Sn), and ca. 500 Hz (^{207}Pb).

Obtaining natural-abundance ^{15}N spectra is difficult because of the low sensitivity. Moreover optimization of the cross-polarization conditions is, in those circumstances, itself a problem. Maximum sensitivity is achieved when the contact time is set at a value to balance the cross-polarization rate and the rate of proton–spin–lattice relaxation in the rotating frame. Although the latter can be measured from ^1H (or even ^{13}C) studies, the former can only be guessed at in the case of a very insensitive

nucleus such as ^{15}N , especially when motional processes may need to be taken into account. The time taken to achieve a signal means that repetition in order to achieve optimization is not feasible. Such considerations help to explain the apparent variability in quality of the ^{15}N spectra. It is hoped to overcome these difficulties in the future by synthesizing ^{15}N -enriched compounds.

For the ^{119}Sn and ^{207}Pb spectra obtained at high spinning speeds, a further difficulty is that of Hartmann-Hahn matching of the proton and metal radio-frequency powers, since rapid spinning makes such matching a more sensitive matter. In practice, however, we experienced little difficulty in this direction, and high-quality metal spectra were obtained in reasonable time with moderate contact times (5 ms).

Acknowledgment. We thank the U.K. Science and Engineering Council for access to the Varian VXR 300 spectrometer under the Solid-state NMR Service arrangements. We are also grateful for financial support from the British Council and the DAAD (Bonn) under the ARC Programme, which enables the international collaboration to take place. A.K.B. and (in part) U.B. wish to thank the Deutsche Forschungsgemeinschaft, Bonn, for financial support, while the Egyptian Ministry of Education kindly contributed with a fellowship (for the deceased T.M.S.) within the framework of the Channel Project.

Registry No. 1, 98104-58-6; 4, 139527-99-4; $[(\text{Bu}_3\text{Sn})_3\text{Co}(\text{CN})_6]$, 64514-55-2; $[\text{H}_3\text{Co}(\text{CN})_6]$, 19528-17-7; $[(\text{Et}_3\text{N})_3\text{Co}(\text{CN})_6]$, 41909-65-3; $[(\text{Et}_3\text{Sn})_3\text{Co}(\text{CN})_6]$, 129264-03-5; $\text{Ag}_3\text{Co}(\text{CN})_6$, 14883-06-8; $\text{K}_3\text{Co}(\text{CN})_6$, 13963-58-1; ^{207}Pb , 14119-29-0; ^{119}Sn , 14314-35-3; ^{59}Co , 7440-48-4.

Supplementary Material Available: Tables with fractional atomic coordinates and temperature factors, significant bond lengths and bond angles, the revised list of coordinates of $(\text{Me}_3\text{Sn})_3\text{Co}(\text{CN})_6$ (based on $P2_1/c$), and general crystal details and references and an ORTEP plot of the asymmetric unit of 4 (6 pages); listings of observed structure factors (12 pages). Ordering information is given on any current masthead page.